HHS Public Access

Author manuscript

Oncogene. Author manuscript; available in PMC 2017 August 30.

Published in final edited form as:

Oncogene. 2009 August 20; 28(33): 2940–2947. doi:10.1038/onc.2009.180.

Interleukin-6 induces an epithelial–mesenchymal transition phenotype in human breast cancer cells

NJ Sullivan[1,2], **AK Sasser**[1,2], **AE Axel**[2], **F Vesuna**[3], **V Raman**[3], **N Ramirez**[2,4], **TM Oberyszyn**[4], and **BM Hall**[1,2]

[1]Integrated Biomedical Science Graduate Program, College of Medicine, The Ohio State University, Columbus, OH, USA

[2]Center for Childhood Cancer, The Research Institute at Nationwide Children's Hospital, Columbus, OH, USA

[3]Department of Radiology, School of Medicine, Johns Hopkins University, Baltimore, MD, USA

[4]Department of Pathology, College of Medicine, The Ohio State University, Columbus, OH, USA

Abstract

Breast tumor interleukin-6 (IL-6) levels increase with tumor grade, and elevated serum IL-6 correlates with poor breast cancer patient survival. Epithelial–mesenchymal transition (EMT) phenotypes such as impaired E-cadherin expression or aberrant Vimentin induction are associated with enhanced metastasis and unfavorable clinical outcome in breast cancer. Despite this fact, few tumor microenvironment-derived extracellular signaling factors capable of provoking such a phenotypic transition have been identified. In this study, we showed that IL-6 promoted E-cadherin repression among a panel of estrogen receptor-α-positive human breast cancer cells. Furthermore, ectopic stable IL-6 expressing MCF-7 breast adenocarcinoma cells (MCF-7^{IL-6}) exhibited an EMT phenotype characterized by impaired E-cadherin expression and induction of Vimentin, N-cadherin, Snail and Twist. MCF-7^{IL-6} cells formed xenograft tumors that displayed loss of E-cadherin, robust Vimentin induction, increased proliferative indices, advanced tumor grade and undifferentiated histology. Finally, we showed aberrant IL-6 production and STAT3 activation in MCF-7 cells that constitutively express Twist, a metastatic regulator and direct transcriptional repressor of E-cadherin. To our knowledge, this is the first study that shows IL-6 as an inducer of an EMT phenotype in breast cancer cells and implicates its potential to promote breast cancer metastasis.

Keywords

interleukin-6; epithelial–mesenchymal transition; breast cancer; tumor microenvironment; metastasis

Correspondence: Associate Professor TM Oberyszyn, Department of Pathology, Ohio State University, 1645 Neil Avenue, 129 Hamilton Hall, Columbus, OH 43210, USA. oberyszyn.1@osu.edu.

Conflict of interest

The authors declare no conflict of interest.

Introduction

Despite recent well-documented molecular and pathological evidence of epithelial–mesenchymal transition (EMT) phenotypes in human breast tumors (Heimann and Hellman, 2000; Moody *et al.*, 2005; Cheng *et al.*, 2008; Sarrio *et al.*, 2008), few tumor microenvironment-derived extracellular cues capable of provoking this transition have been identified. Although EMT comprises a dynamic process critical to metazoan development (Yang and Weinberg, 2008), such phenotypes also promote carcinoma cell invasiveness (Thiery, 2002). In particular, impaired E-cadherin expression in human breast tumors correlates with enhanced invasiveness, metastatic potential (Oka *et al.*, 1993) and decreased breast cancer patient survival (Heimann and Hellman, 2000; Pedersen *et al.*, 2002). Moreover, human breast tumors exhibit increased interleukin-6 (IL-6) expression compared with matched healthy breast tissue, and these IL-6 levels increase with tumor grade (Chavey *et al.*, 2007). Elevated serum IL-6 has been shown in breast cancer patients compared with normal donors (Jiang *et al.*, 2000; Kozlowski *et al.*, 2003) and correlates with advanced breast tumor stage (Kozlowski *et al.*, 2003), increased number of metastatic sites (Salgado *et al.*, 2003) and an overall poor prognosis (Zhang and Adachi, 1999; Bachelot *et al.*, 2003; Salgado *et al.*, 2003).

Normal polarized epithelial cells exhibit ‘cobblestone’ homophilic morphology and express specific proteins, including E-cadherin, cytokeratins, occludins and claudins. However, carcinoma cells may develop a fibro-blastoid morphology and a mesenchymal phenotype characterized by distinct proteins, including Vimentin, N-cadherin, Fibronectin and α-smooth muscle actin (Thiery and Sleeman, 2006). Carcinomas, including breast carcinoma, often present with reduced expression of E-cadherin, a calcium-dependent intercellular adhesion molecule and dominant constituent of epithelial cell adherens junctions. Among other mechanisms, this can be a result of germline mutations, promoter hypermethylation, or aberrantly expressed repressive transcription factors, such as Twist, Snail (SNAI1), Slug (SNAI2), SIP1 or ZEB1 (Yang and Weinberg, 2008).

The role of cytokines in cancer has been well studied (Massague, 2008; Naugler and Karin, 2008), particularly in breast cancer (Nicolini *et al.*, 2006; Chavey *et al.*, 2007). Some cytokines have been shown to induce phenotypes consistent with EMT in transformed epithelial as well as carcinoma cell lines. For example, transforming growth factor-beta1 (TGF-β1) and interleukin-like EMT inducer have independently been shown to promote an EMT phenotype in mouse mammary epithelial cells (Thuault *et al.*, 2006; Waerner *et al.*, 2006). IL-6 is a pleiotropic cytokine that participates in acute inflammation as the major inducer of C-reactive protein, plays a central role in hematopoiesis (Kishimoto, 2006), and enhances proliferation of breast cancer cells (Sasser *et al.*, 2007b). IL-6 signaling utilizes a specific IL-6 receptor (IL-6R/CD126) as well as a promiscuous transmembrane signal transducer, gp130 (CD130), to initiate the Jak/STAT3 pathway.

To our knowledge, this is the first study that shows the induction of an EMT phenotype in carcinoma cells exposed to IL-6. We utilized a three-dimensional (3D) culture assay and an orthotopic xenograft model to show that IL-6 effectively promoted an EMT phenotype in estrogen receptor-alpha (ERα)-positive human breast cancer cells. Specifically, IL-6

exposure induced Vimentin, N-cadherin, Snail and Twist, and repressed E-cadherin. This phenotype was further characterized by enhanced invasiveness *in vitro* and increased tumor cell proliferative index, advanced histological grade and poor differentiation *in vivo*.

Results

IL-6 exposure represses E-cadherin protein expression

We and others have previously shown that ERα-positive human breast cancer cells, including MCF-7, BT474, T47D and ZR-75-1, do not express IL-6 (Sansone *et al.*, 2007; Sasser *et al.*, 2007b). E-cadherin protein levels were assessed after exposure to IL-6 within a 3D culture assay (Sasser *et al.*, 2007a, 2007b), which allowed us to physiologically model the dimensionality and stiffness of *in vivo* mammary tumor microenvironments (Paszek *et al.*, 2005). IL-6 exposure resulted in decreased E-cadherin in MCF-7 cells at 2, 4, 8 and 24 h time points by western blot analysis (Figure 1a). Likewise, BT474, T47D and ZR-75-1 cells showed almost complete abrogation of E-cadherin protein levels at 24 h of IL-6 exposure (Figure 1b).

Autocrine IL-6 expression promotes an EMT phenotype

To characterize the extent to which IL-6 is capable of inducing an EMT phenotype, we evaluated MCF-7 cells that constitutively express ectopic IL-6 (MCF-7^{IL-6}). Quantitative real-time PCR analysis showed a gene expression pattern consistent with EMT including *E-cadherin* repression and concomitant induction of *Vimentin*, *N-cadherin*, *Snail* and *Twist* in MCF-7^{IL-6} cells compared with control cells (Figure 2a). Western blot analysis of MCF-7^{IL-6} cells showed nearly complete abrogation of E-cadherin, which coincided with induction of N-cadherin and Vimentin (Figure 2b). Immunofluorescence microscopy was utilized to compare immunostaining of E-cadherin and Vimentin in MCF-7 control versus MCF-7^{IL-6} cells. MCF-7 control cells showed typical epithelial homophilic adhesion, E-cadherin localization at cell–cell junctions and lacked Vimentin expression. Meanwhile, MCF-7^{IL-6} cells lacked E-cadherin and expressed prominent cytoplasmic Vimentin intermediate filaments (Figure 2c).

IL-6 enhances invasiveness

EMT phenotypes are associated with enhanced tumor cell invasiveness. To determine whether IL-6 exposure functionally enhanced the invasive capacity of MCF-7 cells, an *in vitro* basement membrane extract (BME) invasion assay was utilized. MCF-7 control cells showed minimal invasion through BME in the presence or absence of fetal bovine serum, which served as a chemoattractant. In contrast, MCF-7^{IL-6} cells were significantly (P-value <0.05) more invasive in the presence or absence of FBS, and attained over a 20-fold increase in directional invasiveness toward FBS compared with MCF-7 control cells (Figure 3).

Ectopic twist expression stimulates IL-6 production and STAT3 activation

Constitutive expression of Twist in MCF-7 cells (MCF-7^{Twist}) has been shown to induce a morphology and phenotype consistent with EMT (Mironchik *et al.*, 2005), analogous to those currently noted for MCF-7^{IL-6} cells. Accordingly, we examined cellular supernatants from MCF-7 vector control cells (MCF-7^{vector}) and MCF-7^{Twist} cells for the production of

soluble IL-6 by enzyme-linked immunosorbent assay (ELISA). Although MCF-7^{vector} cells produced an undetectable concentration of IL-6 as expected (Sansone *et al.*, 2007; Sasser *et al.*, 2007b), MCF-7^{Twist} cells produced more than 350 pg/ml of IL-6 (Figure 4a). Therefore, we examined the baseline level of phospho-STAT3^{Y705} in MCF-7^{vector} and MCF-7^{Twist} cells, and only the MCF-7^{Twist} cells displayed aberrantly activated STAT3 (Figure 4b). To determine whether STAT3 was required for the EMT phenotypes in human breast cancer cells, we inhibited STAT3 activation in MCF7^{IL-6} and MCF-7^{Twist} cells with JSI-124, a highly selective small-molecular inhibitor of the Jak/STAT3 signaling pathway (Blaskovich *et al.*, 2003). STAT3 inhibition induced rapid cell death in our cell lines (data not shown), which was corroborated by similar reports in other carcinoma cells (Barton *et al.*, 2004; Lin *et al.*, 2005; Gritsko *et al.*, 2006).

Constitutive IL-6 expression maintains an EMT phenotype and promotes cell proliferation in an orthotopic xenograft model of breast cancer

Tumor sections from all orthotopic xenograft tumors (n=12 xenografts per cell line) were blindly evaluated and graded by a trained pathologist. Microscopic evaluation of a representative section of MCF-7 control tumor showed rare tubule formation (<10% of the tumor, three points), high nuclear grade (three points) and mitotic activity averaging two mitotic figures per high-power field, including abnormal forms (one point). The histological grade of this tumor was 2 (moderately differentiated) based on an overall score of 7. Individual tumor cell necrosis comprising <10% of the tumor was also noted. The tumor cells were strongly immunopositive for membranous E-cadherin and immunonegative for Vimentin. Patchy intracytoplasmic mucin positivity comprised <10% of the tumor and was mostly associated with tubule formation. These results can also be seen in association with moderately differentiated tumors.

Microscopic evaluation of a representative section of MCF-7^{IL-6} tumor showed no tubule formation (three points), high nuclear grade (three points) and mitotic activity averaging eight mitotic figures per high-power field, including abnormal forms (two points). The histological grade of this tumor is 3 (poorly differentiated), based on an overall score of 8. The presence of 10–20% geographic areas of tumor necrosis was noted. E-cadherin was immunonegative, and cytoplasmic immunopositivity for Vimentin was diffuse and strong in the tumor cells. It was also noted that was the absence of intracytoplasmic mucin. These results can also be seen in association with poorly differentiated tumors.

In agreement with our *in vitro* data, MCF-7 control tumors expressed membranous E-cadherin, whereas MCF-7^{IL-6} tumors did not. Vimentin expression was immunonegative in MCF-7 control tumors, but MCF-7^{IL-6} tumors showed robust Vimentin protein expression. Importantly, the human IL-6 receptor does not recognize murine IL-6 (van Dam *et al.*, 1993), and consequently, E-cadherin repression and Vimentin induction are only evident in MCF-7^{IL-6} tumors, as these tumors expressed human IL-6. Consistent with our previously published report of enhanced MCF-7^{IL-6} tumor engraftment and size compared with MCF-7 control tumors (Sasser *et al.*, 2007b), MCF-7^{IL-6} tumors showed more mitotic figures than MCF-7 control tumors by hematoxylin and eosin stain (H&E), suggestive of a higher proliferation rate (Figure 5).

Discussion

Collectively, these data show that IL-6 promotes an EMT phenotype in human breast cancer cells. In particular, we showed IL-6-dependent E-cadherin repression in four ERα-positive human breast cancer cell lines (Figure 1). Likewise, constitutive IL-6 expression induced a gene expression pattern (Figure 2a) and EMT phenotype (Figures 2b and c) in MCF-7^{IL-6} cells. As a functional consequence of IL-6 signaling, MCF-7^{IL-6} cells displayed significantly increased invasiveness when compared with MCF-7 control cells (*P*-value <0.05) (Figure 3). We also showed that ectopic Twist expression in MCF-7 cells induced aberrant IL-6 production (Figure 4a) and constitutive STAT3 activation (Figure 4b). Finally, MCF-7^{IL-6} xenograft tumors exhibited a phenotype consistent with EMT and associated with poor clinical prognosis in breast cancer, which included loss of E-cadherin, Vimentin induction, high mitotic activity, advanced histological grade and poor differentiation (Figure 5).

Although IL-6 is elevated in human breast tumors as well as breast cancer patient sera and associated with a poor prognosis in breast cancer, the source of this IL-6 remains poorly defined. Primary human breast tumor cells (Sansone *et al.*, 2007) and human breast cancer cell lines (Sasser *et al.*, 2007b) are capable of producing autocrine IL-6, suggesting carcinoma cells as a source of aberrantly increased tumor and serum IL-6. We now show that on aberrant IL-6 overexpression, human breast carcinoma cells acquire a more aggressive phenotype. We have also recently shown that primary breast fibroblasts and fibroblasts isolated from common sites of breast cancer metastasis produce IL-6 (Studebaker *et al.*, 2008), which shows one potential mechanism of paracrine IL-6 signaling in human breast cancer. Whether IL-6 signaling in the tumor microenvironment is autocrine-mediated from carcinoma cells or paracrine-mediated from stromal cells, such as fibroblasts, activated immune cells or endothelial cells, we have previously shown that sustained IL-6 signaling constitutively activates STAT3 in human breast cancer cells (Sasser *et al.*, 2007b). A recent study found that STAT3 has the capacity to transactivate *Twist* gene expression (Cheng *et al.*, 2008) and therefore, our current findings suggest that STAT3 may serve as a molecular mediator between IL-6, Twist and ultimate activation of an EMT phenotype in human breast cancer. Furthermore, MCF-7^{Twist} cells aberrantly expressed IL-6 and active STAT3, suggesting evidence of a vicious cycle whereby IL-6 signals through STAT3 to transactivate Twist and subsequently promote autocrine-mediated IL-6 signaling events.

Stromal fibroblasts represent a major cell type within the tumor microenvironment, and soluble factors from mammary carcinoma-associated fibroblasts were shown to induce an EMT phenotype in PMC42-LA human breast carcinoma cells. The authors could not reproduce the phenotype with recombinant proteins known to be present in fibroblast-conditioned medium, including IGF-I, IGF-II (insulin-like growth factor-I, II), TNF-α, VEGF (vascular endothelial growth factor) and TGF-β (Lebret *et al.*, 2007). However, IL-6, a factor produced by human breast fibroblasts (Singh *et al.*, 1999), was not tested. In another relevant study, Karnoub *et al.* (Karnoub *et al.*, 2007) found that bone marrow-derived human mesenchymal stem cells, a predominant population of bone marrow stromal fibroblasts that produces IL-6 (Sasser *et al.*, 2007b), enhanced breast cancer metastasis. Our findings

suggest that IL-6 may be involved in fibroblast-mediated EMT phenotypes and enhanced metastasis in breast cancer.

The IL-6 signaling network has been targeted with several therapeutic antagonists in various human cancer preclinical and clinical trials, but this strategy has yet to be employed for breast cancer. We have shown an IL-6-mediated EMT phenotype in breast cancer cells, which is clinically associated with unfavorable outcome in numerous types of human carcinomas. These data support a potential link between poor breast cancer patient survival associated with high serum IL-6 (Zhang and Adachi, 1999; Jiang *et al.*, 2000; Bachelot *et al.*, 2003; Kozlowski *et al.*, 2003; Salgado *et al.*, 2003) and impaired tumor E-cadherin expression (Oka *et al.*, 1993; Heimann and Hellman, 2000; Pedersen *et al.*, 2002). Although further studies are needed to fully define the role of IL-6 in breast cancer progression and eventual metastasis, our findings strengthen the rationale for evaluation of anti-IL-6 therapies in breast cancer.

Materials and methods

Breast cancer cell lines

The ERα-positive human breast cancer cell lines, MCF-7, BT474, T47D and ZR-75-1, were purchased from the American Type Culture Collection (ATCC, Manassas, VA, USA). MCF-7^{IL-6} cells were provided by Dr Mercedes Rincón (University of Vermont, Burlington, VT, USA) (Conze *et al.*, 2001) andMCF-7^{vector} and MCF-7^{Twist} cells were previously published by Dr Venu Raman (Mironchik *et al.*, 2005). All cell lines were maintained in humidified incubators at 37 °C and 5% CO_2 and cultured in RPMI-1640 medium (Invitrogen, Carlsbad, CA, USA) containing 5% characterized FBS (HyClone, Logan, UT, USA), 2mM L-glutamine, 10 units/ml penicillin and 10 μg/ml streptomycin, hereafter termed complete medium.

Real-time quantitative PCR

Total cellular RNA was isolated using a PureLink Micro-to-Midi Total RNA Purification System (Invitrogen, Carlsbad, CA, USA), and cDNA was synthesized using a RT^2 First Strand Kit (SABiosciences, Frederick, MD, USA). Real-time PCR was performed using RT^2 Real-Time SYBR Green/ROX PCR Master Mix (SABiosciences) on an ABI Prism 7000 Sequence Detection System (Applied Biosystems, Foster City, CA, USA). Data are shown normalized to *GAPDH* expression and averaged between three repeated experiments. Primer sequences were as follows. *E-cadherin*, forward: 5′-CCCACC ACGTACAAGGGTC-3′, reverse: 5′-CTGGGGTATTGGG GGCATC-3′; *N-cadherin*, forward: 5′-CAACTTGCCAGAA AACTCCAGG-3′, reverse: 5′-ATGAAACCGGGCTATCTGCTC-3′; *Vimentin*, forward: 5′-CGCCAGATGCGTGAAATGG-3′, reverse: 5′-ACCAGAGGGAGTGAATCCAGA-3′; *Snail*, forward: 5′-AATCGGAAGCCTAACTACAGCG-3′, reverse: 5′-GTCCCAGATGAGCATTGGCA-3′; *Twist*, forward: 5′-GTCCGCAGTCTTACGAGGAG-3′, reverse: 5′-GCTTGAGGGTCTGAATCTTGCT-3′; *GAPDH*, forward: 5′-GATGCTGGCGCTGAGTACG-3′, reverse: 5′-GCTAAGCAGTTGGTGGTGC-3′.

Western blot analysis

Whole cell lysates were harvested and western blot analysis was performed as described previously (Sasser *et al.*, 2007b). Primary antibodies included rabbit anti-N-cadherin 1:1000 (Santa Cruz Biotechnology, Santa Cruz, CA, USA), rabbit anti-E-cadherin 1:1000 (Cell Signaling, Danvers, MA, USA), mouse anti-Vimentin 1:500 (Clone V9, Dako, Denmark), rabbit anti-phospho-STAT3^{Y705} 1:1000 (Cell Signaling), rabbit anti-STAT3 1:1000 (Cell Signaling) and mouse anti-β-actin 1:10 000 (Clone AC-15, Sigma, St Louis, MO, USA). Secondary antibodies included goat anti-rabbit IgG-HRP 1:1000 (Santa Cruz Biotechnology) and sheep anti-mouse IgG-HRP 1:1000 (GE Healthcare, Chalfont St Giles, UK). All antibodies were diluted with 5% milk in phosphate buffered saline (PBS) containing 0.1% Tween-20 (PBS-T) and incubated for either 1 h at room temperature or overnight at 4 °C. All western blots were visualized with ECL western blotting substrate (Pierce, Rockford, IL, USA).

Immunofluorescence

A total of 1.5×10^5 cells per chamber were plated into Lab-Tek two-chamber slides (Nunc; Thermo Fisher Scientific, Rochester, NY, USA) overnight. The next day, cells were 50–70% confluent, washed one time with PBS, and fixed and permeabilized in cold 100% methanol at −20 °C for 20min. Chambers were given three 5-min washes in 0.1% Tween-20/PBS (PBST) and were then incubated in 3% BSA/0.1% Tween-20/PBS blocking buffer for 1 h at room temperature. After one PBST wash, chambers were incubated with primary antibodies: rabbit anti-E-cadherin 1:200 (Santa Cruz Biotechnology) and mouse anti-Vimentin 1:200 (Dako) in blocking buffer for 2 h at room temperature. Chambers were given three 5-min PBST washes and were then incubated with secondary antibodies: donkey anti-rabbit-Alexa Fluor 594 1:1,000 (Molecular Probes; Invitrogen) and goat anti-mouse-Alexa Fluor 488 1:1,000 (Molecular Probes; Invitrogen) in blocking buffer for 1 h at room temperature in the dark. Secondary antibody alone was used as a negative immunofluorescent control. After three 5-min PBST washes, chambers were incubated with 0.25 μg/ml DAPI (Molecular Probes; Invitrogen) for 1min at room temperature in the dark. Chambers were given three 5-min PBST washes, plastic chamber inserts were removed, and slides were coverslipped with ProLong Gold antifade reagent (Molecular Probes; Invitrogen). Slides were evaluated with a Nikon Eclipse E400 microscope (Melville, NY, USA), and images were taken with a Nikon DXM1200 digital camera using Nikon Act-1 version 2.63 imaging software. Merged images were created with SPOT Advanced version 4.0.9 imaging software (Diagnostic Instruments, Sterling Heights, MI, USA).

Invasion assay

BD Falcon FluoroBlok Cell Culture Inserts for 24-well plates (BD Biosciences, San Jose, CA, USA) were pre-coated with 3 mg/ml Matrigel BME (BD Biosciences) diluted in phenol red-free RPMI-1640 medium (Invitrogen) containing 2mM GlutaMax (Invitrogen), hereafter termed serum-free medium. Breast cancer cells were labeled with 1 μM CFDA-SE (carboxyfluorescein diacetate-succinimidyl ester) (Invitrogen) and then plated in a complete medium overnight. The following day, adherent cells were trypsinized, and 100 000 cells per well were added to a BME-coated 24-well invasion assay plate. Fluorescent cells that had

invaded through the BME layer to the underside of the insert were counted at 20 h. Assay was repeated to confirm.

3D culture assay

Cultrex BME (Trevigen, Gaithersburg, MD, USA) was diluted in serum-free medium and plated at a concentration of 6 mg/ml per well into a 24-well plate and allowed to solidify for a minimum of 1h at 37°C. All cells were harvested with CellStripper non-enzymatic cell dissociation solution (Mediatech, Manassas, VA, USA) according to the manufacturer's protocol to prevent trypsin-mediated E-cadherin cleavage between standard 2D culture and 3D assays. For 24 h 3D studies, 250 000 cells embedded in 3 mg/ml BME with or without 50 ng/ml recombinant human IL-6 (Peprotech, Rocky Hill, NJ, USA) were plated per well. Cells were harvested at each time point by dilution with serum-free medium, centrifugation out of BME suspension and lysed with SDS (sodium dodecyl sulfate) lysis buffer (62.5mM Tris-HCl, 2%w/v SDS, 10% glycerol, 50 nM DTT and 0.01%w/v bromophenol blue). For 2-week MCF-7 3D studies, 150 000 cells were plated per well and harvested as described for 24 h 3D studies with one exception. At day 7, a sample of IL-6-treated cells was harvested from BME and expanded in the absence of IL-6 for another 7 days of 3D culture. Western blot analysis was performed as described above.

Quantification of soluble IL-6 protein

A total of 750 000 cells were plated into a 6-well plate and allowed to adhere overnight. The next day, cells were washed once with PBS and 1ml complete medium was added gently. Cells were allowed to grow for 48 h, at which time cellular supernatants were harvested and 0.2 μm filtered. Supernatants were assayed for soluble IL-6 protein using the Human IL-6 DuoSet ELISA Development Kit (R&D Systems, Minneapolis, MN, USA) according to the manufacturer's protocol. Data are shown averaged between two repeated experiments.

Xenografts, histopathology and immunohistochemistry

Immunocompromised athymic nude (nu/nu) female mice were purchased at 3–4 weeks of age (The Jackson Laboratory, Bar Harbor, ME, USA). A total of 2×10^6 MCF-7 control or MCF-7^{IL-6} cells suspended in 6 mg/ml Cutlrex BME (Trevigen) were orthotopically injected into the fifth and tenth mammary fat pad of six mice per group (n=12 xenografts per cell line). Tumors were resected at 6 weeks, formalin-fixed and paraffin-embedded using the standard methods.

Xenograft tissue sections of MCF-7 control and MCF-7^{IL-6} tumors were blindly evaluated microscopically for proliferative indices and degree of differentiation using H&E and mucicarmine stained sections, respectively. E-cadherin and Vimentin protein expressions were also evaluated by IHC (immunohistochemistry). The H&E stained tumors were graded using the Nottingham combined histological grading system (Elston–Ellis modification of the Scarff–Bloom–Richardson grading system) for invasive breast cancers, which includes evaluation of morphological features, such as tubule formation, nuclear pleomorphism and mitotic count (Elston and Ellis, 1991). Mitotic counts were averaged on evaluation of five separate high-power fields.

Thin 5 μm tissue sections from the surface of tissue blocks were mounted onto glass slides, stained with H&E and coverslipped in the usual manner. A second set of thin tissue sections were mounted onto glass slides, stained with mucicarmine using the standard method and coverslipped in the usual manner. Immunoperoxidase staining was performed on a third set of thin tissue sections, placed onto charged slides and deparaffinized. Slides were then immersed in Antigen Retrieval Citra Solution (BioGenex, San Ramon, CA, USA) in a pressure cooker at 120 °C, blocked in Power Block Universal Blocking Reagent (BioGenex) for 10 min at room temperature, and washed one time with PBS. Primary antibodies were diluted in Power Block reagent. Slides were incubated with rabbit anti-E-cadherin 1:50 (Cell Signaling) or mouse anti-Vimentin 1:200 (Clone V9, Dako) primary antibody overnight at 4 °C and subsequently washed three times with Super Sensitive Wash Buffer (BioGenex). Slides were then incubated with 1 × Universal Link biotinylated goat anti-mouse and rabbit IgG secondary antibody (Biocare Medical, Concord, CA, USA) for 10 min at room temperature, washed three times with wash buffer, and incubated with streptavadin-HRP (Biocare Medical) in the dark for 30 min at room temperature. After three wash buffer washes, AEC substrate chromogen (Dako) was added, and the IHC sections were coverslipped in the usual manner. All experiments involving animals were conducted in accordance with The Research Institute at Nationwide Children's Hospital Institutional Animal Care and Usage Committee (IACUC).

Statistical analysis

Student's *t*-test was performed to determine statistically significant differences between groups, and a *P*-value <0.05 was considered significant.

Acknowledgments

This work was funded by the generous support of the Elsa U Pardee Foundation (BH), the American Cancer Society-Ohio Division (BH) and The Research Institute at Nationwide Children's Hospital (BH).

References

Bachelot T, Ray-Coquard I, Menetrier-Caux C, Rastkha M, Duc A, Blay JY. Prognostic value of serum levels of interleukin 6 and of serum and plasma levels of vascular endothelial growth factor in hormone-refractory metastatic breast cancer patients. Br J Cancer. 2003; 88:1721–1726. [PubMed: 12771987]

Barton BE, Karras JG, Murphy TF, Barton A, Huang HF. Signal transducer and activator of transcription 3 (STAT3) activation in prostate cancer: direct STAT3 inhibition induces apoptosis in prostate cancer lines. Mol Cancer Ther. 2004; 3:11–20. [PubMed: 14749471]

Blaskovich MA, Sun J, Cantor A, Turkson J, Jove R, Sebti SM. Discovery of JSI-124 (cucurbitacin I), a selective Janus kinase/signal transducer and activator of transcription 3 signaling pathway inhibitor with potent antitumor activity against human and murine cancer cells in mice. Cancer Res. 2003; 63:1270–1279. [PubMed: 12649187]

Chavey C, Bibeau F, Gourgou-Bourgade S, Burlinchon S, Boissiere F, Laune D, et al. Oestrogen receptor negative breast cancers exhibit high cytokine content. Breast Cancer Res. 2007; 9:R15. [PubMed: 17261184]

Cheng GZ, Zhang WZ, Sun M, Wang Q, Coppola D, Mansour M, et al. Twist is transcriptionally induced by activation of STAT3 and mediates STAT3 oncogenic function. J Biol Chem. 2008; 283:14665–14673. [PubMed: 18353781]

Conze D, Weiss L, Regen PS, Bhushan A, Weaver D, Johnson P, et al. Autocrine production of interleukin 6 causes multidrug resistance in breast cancer cells. Cancer Res. 2001; 61:8851–8858. [PubMed: 11751408]

Elston CW, Ellis IO. Pathological prognostic factors in breast cancer. I. The value of histological grade in breast cancer: experience from a large study with long-term follow-up. Histopathology. 1991; 19:403–410. [PubMed: 1757079]

Gritsko T, Williams A, Turkson J, Kaneko S, Bowman T, Huang M, et al. Persistent activation of stat3 signaling induces survivin gene expression and confers resistance to apoptosis in human breast cancer cells. Clin Cancer Res. 2006; 12:11–19. [PubMed: 16397018]

Heimann R, Hellman S. Individual characterisation of the metastatic capacity of human breast carcinoma. Eur J Cancer. 2000; 36:1631–1639. [PubMed: 10959049]

Jiang XP, Yang DC, Elliott RL, Head JF. Reduction in serum IL-6 after vacination of breast cancer patients with tumour-associated antigens is related to estrogen receptor status. Cytokine. 2000; 12:458–465. [PubMed: 10857759]

Karnoub AE, Dash AB, Vo AP, Sullivan A, Brooks MW, Bell GW, et al. Mesenchymal stem cells within tumour stroma promote breast cancer metastasis. Nature. 2007; 449:557–563. [PubMed: 17914389]

Kishimoto T. Interleukin-6: discovery of a pleiotropic cytokine. Arthritis Res Ther. 2006; 8:S2.

Kozlowski L, Zakrzewska I, Tokajuk P, Wojtukiewicz MZ. Concentration of interleukin-6 (IL-6), interleukin-8 (IL-8) and interleukin-10 (IL-10) in blood serum of breast cancer patients. Rocz Akad Med Bialymst. 2003; 48:82–84. [PubMed: 14737948]

Lebret SC, Newgreen DF, Thompson EW, Ackland ML. Induction of epithelial to mesenchymal transition in PMC42-LA human breast carcinoma cells by carcinoma-associated fibroblast secreted factors. Breast Cancer Res. 2007; 9:R19. [PubMed: 17311675]

Lin Q, Lai R, Chirieac LR, Li C, Thomazy VA, Grammatikakis I, et al. Constitutive activation of JAK3/STAT3 in colon carcinoma tumors and cell lines: inhibition of JAK3/STAT3 signaling induces apoptosis and cell cycle arrest of colon carcinoma cells. Am J Pathol. 2005; 167:969–980. [PubMed: 16192633]

Massague J. TGFbeta in cancer. Cell. 2008; 134:215–230. [PubMed: 18662538]

Mironchik Y, Winnard PT Jr, Vesuna F, Kato Y, Wildes F, Pathak AP, et al. Twist overexpression induces *in vivo* angiogenesis and correlates with chromosomal instability in breast cancer. Cancer Res. 2005; 65:10801–10809. [PubMed: 16322226]

Moody SE, Perez D, Pan TC, Sarkisian CJ, Portocarrero CP, Sterner CJ, et al. The transcriptional repressor Snail promotes mammary tumor recurrence. Cancer Cell. 2005; 8:197–209. [PubMed: 16169465]

Naugler WE, Karin M. The wolf in sheep's clothing: the role of interleukin-6 in immunity, inflammation and cancer. Trends Mol Med. 2008; 14:109–119. [PubMed: 18261959]

Nicolini A, Carpi A, Rossi G. Cytokines in breast cancer. Cytokine Growth Factor Rev. 2006; 17:325–337. [PubMed: 16931107]

Oka H, Shiozaki H, Kobayashi K, Inoue M, Tahara H, Kobayashi T, et al. Expression of E-cadherin cell adhesion molecules in human breast cancer tissues and its relationship to metastasis. Cancer Res. 1993; 53:1696–1701. [PubMed: 8453644]

Paszek MJ, Zahir N, Johnson KR, Lakins JN, Rozenberg GI, Gefen A, et al. Tensional homeostasis and the malignant phenotype. Cancer Cell. 2005; 8:241–254. [PubMed: 16169468]

Pedersen KB, Nesland JM, Fodstad O, Maelandsmo GM. Expression of S100A4, E-cadherin, alpha- and beta-catenin in breast cancer biopsies. Br J Cancer. 2002; 87:1281–1286. [PubMed: 12439718]

Salgado R, Junius S, Benoy I, Van Dam P, Vermeulen P, Van Marck E, et al. Circulating interleukin-6 predicts survival in patients with metastatic breast cancer. Int J Cancer. 2003; 103:642–646. [PubMed: 12494472]

Sansone P, Storci G, Tavolari S, Guarnieri T, Giovannini C, Taffurelli M, et al. IL-6 triggers malignant features in mammospheres from human ductal breast carcinoma and normal mammary gland. J Clin Invest. 2007; 117:3988–4002. [PubMed: 18060036]

Sarrio D, Rodriguez-Pinilla SM, Hardisson D, Cano A, Moreno-Bueno G, Palacios J. Epithelial–mesenchymal transition in breast cancer relates to the basal-like phenotype. Cancer Res. 2008; 68:989–997. [PubMed: 18281472]

Sasser AK, Mundy BL, Smith KM, Studebaker AW, Axel AE, Haidet AM, et al. Human bone marrow stromal cells enhance breast cancer cell growth rates in a cell line-dependent manner when evaluated in 3D tumor environments. Cancer Lett. 2007a; 254:255–264. [PubMed: 17467167]

Sasser AK, Sullivan NJ, Studebaker AW, Hendey LF, Axel AE, Hall BM. Interleukin-6 is a potent growth factor for ER-alpha-positive human breast cancer. FASEB J. 2007b; 21:3763–3770. [PubMed: 17586727]

Singh A, Purohit A, Ghilchik MW, Reed MJ. The regulation of aromatase activity in breast fibroblasts: the role of interleukin-6 and prostaglandin E2. Endocr Relat Cancer. 1999; 6:139–147. [PubMed: 10731102]

Studebaker AW, Storci G, Werbeck JL, Sansone P, Sasser AK, Tavolari S, et al. Fibroblasts isolated from common sites of breast cancer metastasis enhance cancer cell growth rates and invasiveness in an interleukin-6-dependent manner. Cancer Res. 2008; 68:9087–9095. [PubMed: 18974155]

Thiery JP. Epithelial–mesenchymal transitions in tumour progression. Nat Rev Cancer. 2002; 2:442–454. [PubMed: 12189386]

Thiery JP, Sleeman JP. Complex networks orchestrate epithelial–mesenchymal transitions. Nat Rev Mol Cell Biol. 2006; 7:131–142. [PubMed: 16493418]

Thuault S, Valcourt U, Petersen M, Manfioletti G, Heldin CH, Moustakas A. Transforming growth factor-beta employs HMGA2 to elicit epithelial–mesenchymal transition. J Cell Biol. 2006; 174:175–183. [PubMed: 16831886]

van Dam M, Mullberg J, Schooltink H, Stoyan T, Brakenhoff JP, Graeve L, et al. Structure-function analysis of interleukin-6 utilizing human/murine chimeric molecules. Involvement of two separate domains in receptor binding. J Biol Chem. 1993; 268:15285–15290. [PubMed: 8325898]

Waerner T, Alacakaptan M, Tamir I, Oberauer R, Gal A, Brabletz T, et al. ILEI: a cytokine essential for EMT, tumor formation, and late events in metastasis in epithelial cells. Cancer Cell. 2006; 10:227–239. [PubMed: 16959614]

Yang J, Weinberg RA. Epithelial–mesenchymal transition: at the crossroads of development and tumor metastasis. Dev Cell. 2008; 14:818–829. [PubMed: 18539112]

Zhang GJ, Adachi I. Serum interleukin-6 levels correlate to tumor progression and prognosis in metastatic breast carcinoma. Anticancer Res. 1999; 19:1427–1432. [PubMed: 10365118]

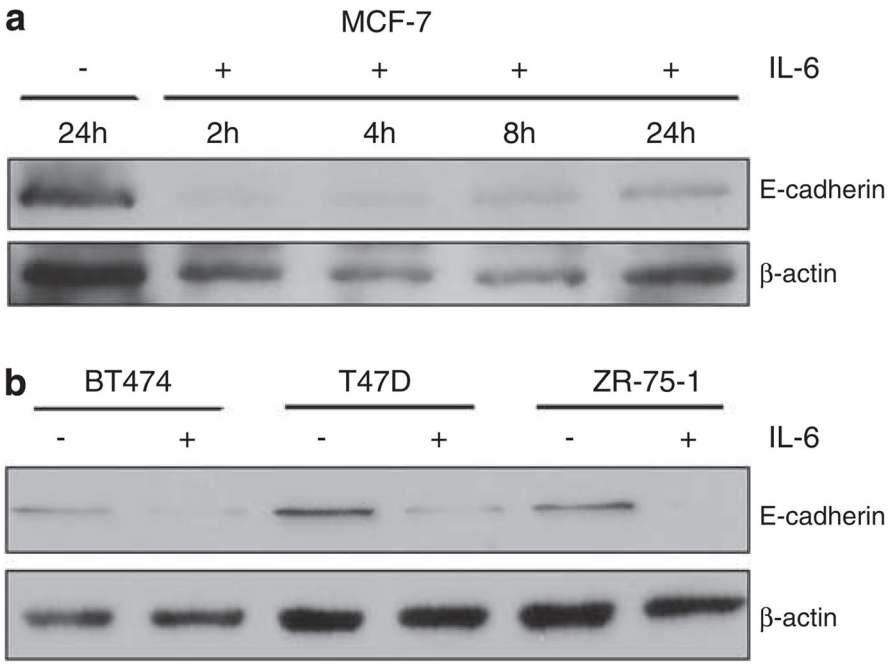

Figure 1.

IL-6 induces E-cadherin protein repression. (**a)** Western blot analysis of MCF-7 cells exposed to 50 ng/ml IL-6 in a 3D culture assay showed a decrease in E-cadherin levels at 2, 4, 8 and 24 h compared with untreated cells in the 3D assay. (**b)** BT474, T47D and ZR-75-1 cells were exposed to 50 ng/ml IL-6 for 24 h in a 3D culture assay, and western blot analysis showed almost complete abrogation of E-cadherin compared with untreated cells.

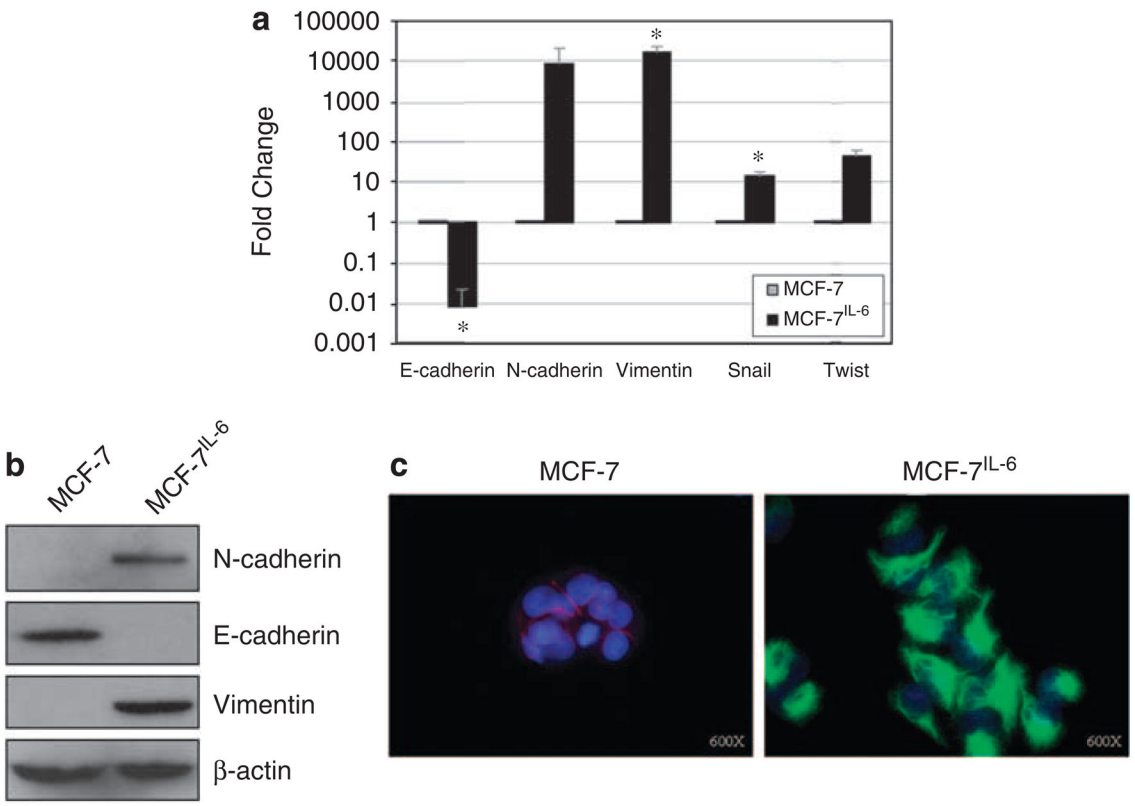

Figure 2.

Constitutive IL-6 expression promotes a gene expression pattern and phenotype consistent with EMT. (**a**) Real-time quantitative PCR analysis of MCF-7^{IL-6} cells showed a robust decrease in *E-cadherin* (**P*-value=0.00003) gene expression and concomitant increase in *N-cadherin*, *Vimentin* (**P*-value < 0.05), *Snail* (**P*-value < 0.05) and *Twist*. Real-time PCR data are shown normalized to *GAPDH* expression and on a logarithmic scale. (**b**) Western blot analysis of MCF-7^{IL-6} cells showed the induction of N-cadherin and Vimentin and abrogation of E-cadherin. (**c**) Immunofluorescent staining of MCF-7 control cells showed normal immunopositive E-cadherin (red; Alexa Fluor 594) localization and no detectable Vimentin (green; Alexa Fluor 488). Conversely, MCF-7^{IL-6} cells exhibited no detectable E-cadherin and strong immunopositive staining for Vimentin. DAPI nuclear stain is shown in blue.

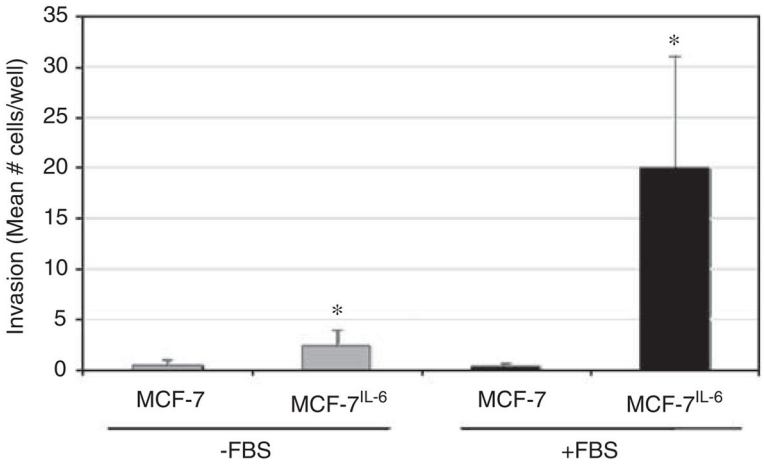

Figure 3.

IL-6 expression enhances invasiveness *in vitro*. MCF-7 control cells showed minimal invasion through BME both with (black bars) and without (gray bars) the addition of FBS as a chemoattractant. In contrast, MCF-7^{IL-6} cells showed significantly (*P-value < 0.05) increased invasiveness, particularly with FBS supplementation.

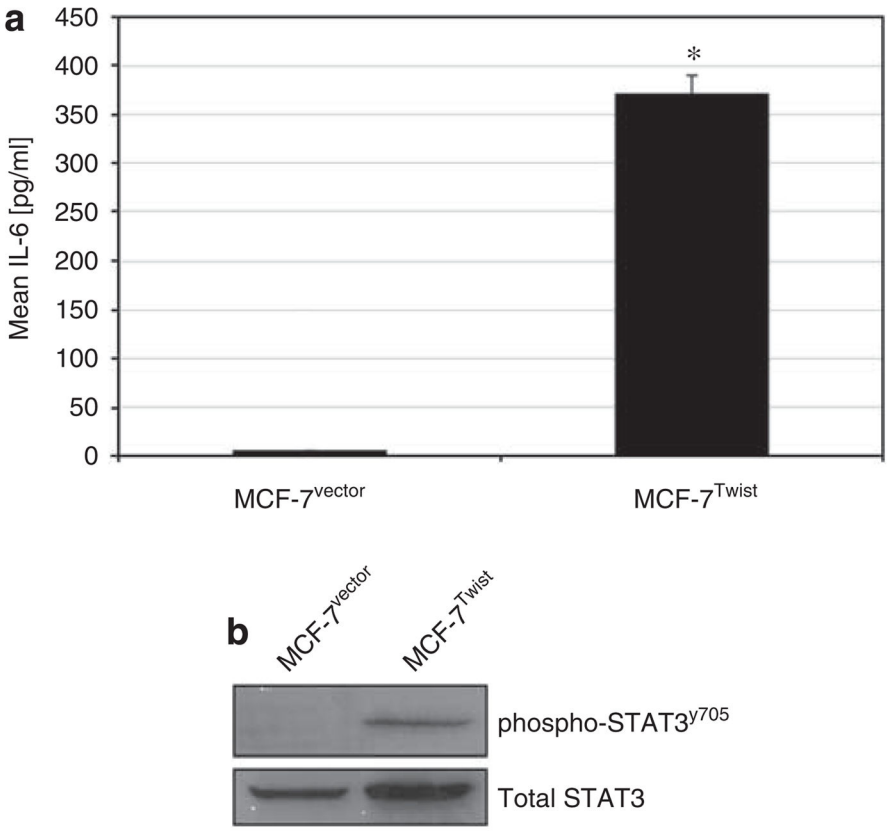

Figure 4.

Ectopic Twist expression stimulates secretion of IL-6 and constitutive STAT3 activation. (**a**) 48 h cellular supernatants were assessed by enzyme-linked immunosorbent assay and showed no detectable soluble IL-6 production in MCF-7^{vector} cells compared with greater than 350 pg/ml IL-6 in MCF-7^{Twist} cells (*P-value=0.01). (**b**) MCF-7^{Twist} cells expressed elevated phosphorylated $STAT3^{Y705}$ (phospho-$STAT3^{Y705}$) as shown by western blot analysis.

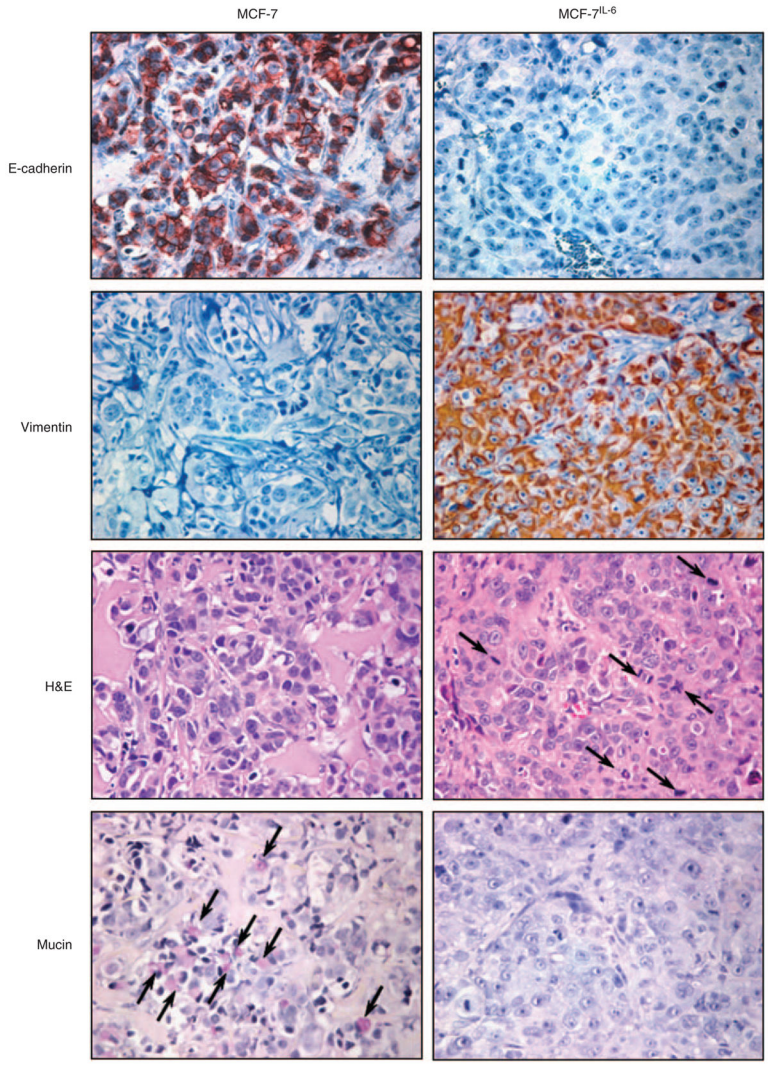

Figure 5.

Autocrine IL-6 production maintains an EMT phenotype in orthotopic xenograft tumors. 2×10^6 BME-embedded cancer cells were orthotopically injected into the fifth and tenth mammary fat pad of six mice per group (n=12 xenografts per cell line), and tumors were resected at 6 weeks. Tumors shown are representative of all stained tumor sections in that group. E-cadherin expression was immunopositive and localized at intercellular junctions in MCF-7 control tumors and immunonegative in MCF-7^{IL-6} tumors. Vimentin expression was immunonegative in MCF-7 control tumors and highly immunopositive in MCF-7^{IL-6} tumors. H&E staining showed increased mitotic figures (arrows) in MCF-7^{IL-6} tumors compared with MCF-7 control tumors. Mucicarmine staining showed focal expression of mucin in MCF-7 control tumors (arrows), suggestive of better differentiated MCF-7 cells within these xenografts. MCF-7^{IL-6} tumors lacked mucin, suggestive of poorly differentiated MCF-7 cells within these xenografts.